Available online at www.CivileJournal.org

Civil Engineering Journal

(E-ISSN: 2476-3055; ISSN: 2676-6957)

Vol. 10, Special Issue, 2024

"Sustainable Infrastructure and Structural Engineering: Innovations in Construction and Design"

Comparison of Structural Response Utilizing Probabilistic Seismic Hazard Analysis and Design Spectral Ground Motion

Pranowo [1*], Lalu Makrup [1*], Widodo Pawirodikromo [1], Yunalia Muntafi [1]

[1] *Department of Civil Engineering, Universitas Islam Indonesia, Yogyakarta, Indonesia.*

Received 15 September 2024; Revised 23 November 2024; Accepted 07 December 2024; Published 16 December 2024

Abstract

Indonesia is seismically active due to tectonic plate convergence south of Java Island. In the examination of earthquake-resistant structures, Indonesia possesses the SNI 1726-2019 rule; however, it requires re-evaluation in conjunction with other seismic motions, specifically the PSHA method. The PSHA approach is employed in probability-based seismic hazard analysis, taking into account uncertainties related to earthquake magnitude, location, and frequency to provide a comprehensive assessment of a location's hazard level. To demonstrate the impact of ground motion induced by earthquakes on structural reaction, it is essential to study the structure using the time history of SNI and PSHA artificial earthquake shaking. Spectrum matching with target spectra derived from probabilistic seismic hazard analysis can build artificial time histories. Consequently, the time history obtained from the analysis can be considered to be derived from the probabilistic methodology. Both analytical methods, SNI and PSHA, indicate that the structural reaction of the Alana Hotel is not markedly different, and the structure remains secure against seismic activity.

Keywords: Ground Motion; Time History; Probabilistic; Structure Response.

1. Introduction

Seismic loads on multi-story structures can be derived directly from SNI or generated by probabilistic methods to simulate artificial earthquake loads. These two analytical methods provide an overview of the seismic force magnitude to be considered in the design of earthquake-resistant structures. In order to obtain a comprehensive picture of the hazard level of a location under consideration, the Probabilistic Seismic Hazard Analysis (PSHA) method uses the definition of a probability distribution function, which takes into account and combines the uncertainty of the scale of earthquake events, location, and frequency of occurrence. The SNI method utilizes standard regulations in Indonesia to determine earthquake hazard levels. This allows for the analysis of existing earthquake vibrations, which take the form of a spectrum response. It then compares this spectrum response graph to a time history graph, propagating it to the ground level.

Seismic waves will reach a certain location identified as the research site. Seismic ground vibrations at the site are necessary to assess a building structure for seismic loads. SNI and probabilistic methods can determine the ground motion at a site. Probabilistic ground motion time histories and SNI will be constructed for the Alana Hotel building in Yogyakarta, Indonesia, as seen in Figure 1. Figure 2 exemplifies a time history of earthquake ground motion.

* Corresponding author: omprans@yahoo.com; 885110106@uii.ac.id

http://dx.doi.org/10.28991/CEJ-SP2024-010-012

Figure 1. Alana Hotel Building, Yogyakarta, Indonesia

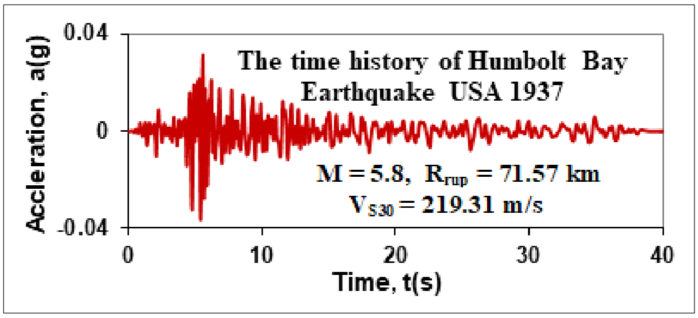

Figure 2. The time history of the Humbolt Bay earthquake (1937)

To generate ground motion (seismic ground motion time history) and assess structural integrity, numerous experts have undertaken research on the subject. Saputro [1] conducted an investigation to establish an artificial time history in bedrock using probabilistic seismic hazard investigation (PSHA). From the bedrock to the earth's surface, the temporal history forms the basis for structural analysis, which evaluates the structural response. Pawirodikromo [2] investigated earthquake vibrations with low, medium, and high A/V ratios to explore the normalization of hysteretic energy and its significance in the damage index of Single Degree of Freedom buildings that displayed inelastic responses during earthquakes. Utomo [3] generated a simulated earthquake in the field to assess the structural response. Widodo [4] utilized earthquake records, including low, medium, and high frequency, to evaluate reinforced concrete frame structures and found a correlation between performance level, deviation, and damage index. Bayati & Sultoni [5] deterministically modified the frequency characteristics of the time history and used it for the seismic design of reinforced concrete frames. Irsyam & Hendriyawan [6] constructed the time history at the bedrock and then propagated it to the Earth's surface to evaluate the gas tank of Indonesia's national electricity company. Pawirodikromo et al. [7] generated ground motions using the Probabilistic Seismic Hazard Assessment (PSHA) and the spectrum matching technique, with the aim of analyzing the directional and directivity effects of synthetic ground motion at a specified site in Yogyakarta. Artati [8] generated simulated earthquake vibrations utilizing the PSHA and SNI methodologies in the Palu region of South Sulawesi to examine the possible risk of liquefaction. The results indicated no significant variations in the recorded earthquake vibrations. Nugroho et al. [9] evaluated building structures utilizing the SNI 1726-2019 spectral response; the results demonstrate that the structural response complies with the required drift ratio limits.

Rocky [10] Conducted an examination of simulated earthquake vibrations utilizing the PSHA method in the new capital region of Indonesia. The focus of this research is on acquiring artificial earthquake vibrations for structural analysis. This research will be intriguing to do, given there has been no comparative analysis of the structural response to ground motion based on SNI and PSHA. In accordance with the 2019 Indonesian National Standard (SNI) [11] and spectral matching methodologies, this study will derive a time history of ground motion at the surface from Probabilistic Seismic Hazard Assessment (PSHA) in bedrock, with a 2% likelihood of exceedance over 50 years. The period's history serves as a basis for structural analysis to assess the building structure of the Alana Hotel, Yogyakarta, Indonesia.

2. Research Methodology

The study methodology involves performing a literature evaluation of prior studies to identify gaps that have not been addressed by previous researchers. The initial step involves gathering data on tall structures in Yogyakarta, including soil investigation data, planning drawings, and the location coordinates of the building sites. The next phase involves modeling the building structure utilizing the Perform 3D Program, incorporating relevant parameters such as element dimensions, floor count, building height, and operational loads. The third phase involves generating an artificial earthquake using the probabilistic method and SNI, represented as time history, to simulate vibrations in tall buildings. The final phase entails analyzing the Perform 3D Program with the aforementioned data inputs to derive the building's response output. Figure 3 provides a brief illustration of the process.

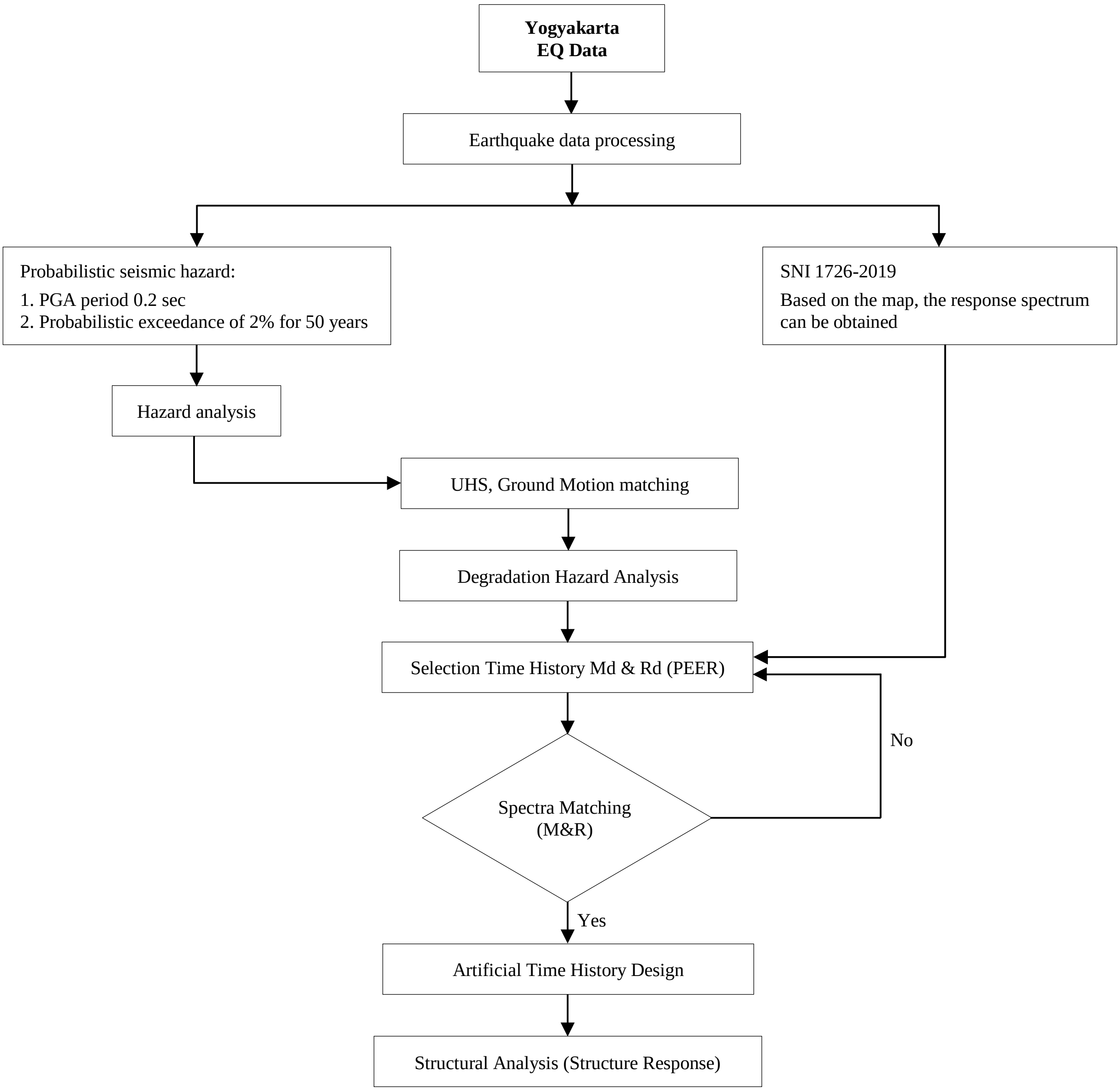

Figure 3. Research flowchart

3. Earthquake Wave and Structural Analysis

Earthquake waves refer to the time history of the acceleration of earthquake waves that occur at a particular location. To see the effect of structural response to earthquake acceleration waves, structural analysis theory is used. We need a set of time histories to document the ground conditions at the site. The structural analysis for the twelve-storey building of Alana Hotel, Yogyakarta, Indonesia, uses the time history as data. Equation 1 is the result of the structural analysis.

$$[M]\{\ddot{X}\} + [C]\{\dot{X}\} + [K]\{X\} = -[\mathrm{M}]a_G \tag{1}$$

In this context, [M], [C], and [K] represent the mass, damping, and stiffness matrices, respectively, whereas $\{\ddot{X}\}$, $\{\dot{X}\}$, and {X} denotes the vectors of acceleration, velocity, and displacement. Additionally, a_G signifies the acceleration time history of an earthquake, calculated using a probabilistic method. The Structural Analysis Program (SAP) is a software application that has formulated Equation 1. This research was conducted using the Perform 3D software

4. Probabilistic Seismic Hazard Analysis (PSHA)

The probabilistic approach enables a clear assessment of uncertainty regarding the site, position, and frequency of earthquakes, together with variations in ground motion patterns associated with earthquake magnitude and location, in evaluating their potential hazards. The framework of probabilistic seismic risk analysis facilitates the identification, quantification, and logical integration of these uncertainties, leading to a more thorough comprehension of seismic hazards. According to Kramer (1996) [12], the likelihood that a ground motion parameter A will surpass a specified value for a given earthquake event can be calculated using the total probability theorem, as expressed in Equation 2.

$$P_A(a) = \int_M \int_R P(A > a)|m,r) f_M(m) f_R(r) dr dm \tag{2}$$

The probability distribution $P(A>a|m,r)$ indicates the likelihood that a ground motion parameter A, which follows a log-normal distribution, will surpass a specific value a. $f_M(m)$ represents the probability distribution of earthquake magnitude, typically modelled as an exponential distribution initially proposed by Gutenberg & Richter [13], and $f_R(r)$ represents the relative probability distribution of distance. Solving Equation 2 analytically is exceedingly difficult, bordering on impossible. Consequently, a numerical solution to the equation is necessary. In this instance, PSHA will be calculated with a 2% probability of exceedance (PE) over a 50-year period.

4.1. Probability of Seismic Parameter Will be Exceeded

Probability of seismic parameter *"a"* will be exceeded by *"A"* where *"a"* and *"A"* are earthquake ground motion acceleration can be written in terms of $P(A>a)$. The statistical distribution subject, represented by the log normal distribution, follows P(A>a). The log normal distribution's density function is represented as follows:

$$p_A(a) = \frac{1}{a\sigma_{\ln A}\sqrt{2\pi}} e^{-\left(\frac{(\ln a - \ln A)^2}{2\sigma^2_{\ln A}}\right)} \tag{3}$$

The Ground Motion Prediction Equation (GMPE) yields ln A. The log-normal distribution has the following cumulative distribution Equation 4:

$$P_A(a) = \int \frac{1}{a\sigma_{\ln A}\sqrt{2\pi}} e^{-\left(\frac{(\ln a - \ln A)^2}{2\sigma^2_{\ln A}}\right)} da \tag{4}$$

According to PSHA calculation so the Equation 4 can be written as Equation 5.

$$P(A > a|m,r) = \int \frac{1}{a\sigma_{\ln A}\sqrt{2\pi}} e^{-\left(\frac{(\ln a - \ln A)^2}{2\sigma^2_{\ln A}}\right)} da \tag{5}$$

The earthquake acceleration *(A)* is contingent upon the earthquake's magnitude *(m)* and the distance from the epicenter to the location *(r).* This research utilizes Ground Motion Prediction Equations (GMPEs) from Sadigh et al. [14], Youngs et al. [15] and Boor & Atkinson [16] to evaluate seismic hazards.

4.2. Magnitude Probability Distribution

PSHA requires the magnitude distribution *fM(m)*, and the development of this distribution began with Gutenberg-Richter's law [13], Equation 6.

$$\lambda_m = 10^{a - b\,m} \quad \text{or} \quad \lambda_m = e^{\alpha - \beta m} \tag{6}$$

where λ_m is the annual event frequency, a and b represent regression constants ascertainable by statistical methods, with parameter a being $\alpha \approx 2.303a$, $\beta \approx 2.303b$. We can incorporate a truncated-below magnitude m_0 into the preceding formulation (Equation 6) to exclude small magnitudes that engineering analysis may neglect. In the majority of hazard evaluations, m_0 generally ranges from 3 to 5, as per the Electric Power Research Institute (EPRI) [17]. Consequently, we can extract the probability density function from Equation 6 as follows:

$$f_M(m) = \beta\, e^{-\beta(m - mo)} \tag{7}$$

Equation 7 facilitates the computation of probability for exceedingly large magnitudes, referred to as unrealistic magnitudes. We establish an upper bound magnitude, m_u, to resolve this issue. It is characterized as the most significant earthquake anticipated to transpire along an active fault line. Nikolaou [18] and Cornell & Vanmarcke [19] suggest a modification to the original Gutenberg-Richter curve, incorporating m_u in addition to the previously considered m_0. The true value of mu must be ascertained through a geological survey of the area, which will yield data regarding the maximum fault rupture and hence the maximum energy and magnitude that can be generated. The comprehensive probability density function $f_M(m)$ for the magnitude range is articulated as:

$$f_M(m) = \frac{\beta e^{-\beta(m - m_0)}}{1 - e^{-\beta(m_u - m_0)}} \text{ with } m_0 < m < m_u \tag{8}$$

The Equation 8 is referred to as a truncated exponential distribution function. Geological and seismological investigations of various faults have demonstrated that sources frequently generate significant earthquakes approaching their maximum magnitude, referred to as typical earthquakes. The phenomenon of the fault segment exhibiting uniform displacement during each seismic event, referred to as the constant fault slip rate, elucidates this observation. The preceding paragraph's referenced exponential model, exclusively based on historical data, underrepresents the frequency of significant earthquakes compared to geological evidence. Youngs & Coppersmith [19] propose an alternate recurrence rule to address the seismicity and frequency of significant events. We denote their model as the characteristic earthquake recurrence law. This method results in the cumulative distribution function becoming flattened near the maximum magnitude. This model integrates a truncated exponential Gutenberg-Richter model for lower magnitudes and a uniform distribution around the maximum magnitude in the probability density function.

$$f_M(m) = \frac{\beta e^{-\beta(m-m_0)}}{1-e^{-\beta(m_u-m_0)}} \quad \text{with } m_0 < m < m_u - ½ \tag{9}$$

$$f_M(m) = \frac{\beta e^{-\beta(m_u-\frac{3}{2}-m_0)}}{1-e^{-\beta(m_u-m_0)}} \quad \text{with } m_u - ½ < m < m_u \tag{10}$$

The PSHA uses the recurrence principles of Gutenberg & Richter [13], Youngs & Coppersmith [20] to delineate the aleatory uncertainty in magnitude distribution.

4.3. Total Probability Theorem Solution and Distance Probability Distribution

A rupture and its intensity may occur at different times and locations along a fault plane. Thus, the occurrence of the rupture can likely be depicted as the predominant portion of the overlapping rupture region along the entire fault plane. Evaluate all equations related to the total probability theorem about the fault plane (i.e., within each rupture zone). The likelihood of a fault rupture is similar to the probability *fR(r)* of the earthquake's rupture-to-site distance (Equation 11).

$$f_R(r) = \frac{a\ rupture\ area}{total\ rupture\ area} \tag{11}$$

In Probabilistic Seismic Hazard Assessment (PSHA), specialists typically employ a rupture width that is equivalent to the rupture length, as noted by McGuire [21]. Consequently, Equation 11 produces a rupture length and width of L for the identical magnitude. Consequently, all future events on a fault with a certain magnitude provide a probability distribution of flattening distance.

4.4. Probability of Seismic Parameter to be Exceeded

The probability that a ground motion parameter A will surpass a specific value *a*, denoted as *P(A>a|m,r)*, is based on the assumption that the data is log-normally distributed or that the logarithm of the data follows a normal (Gaussian) distribution. Probabilistic seismic hazard analysis indicates the standard normal deviation (z*) of the ground motion parameter, as referenced in Equations 3 to 5. The expression for z* is:

$$z^* = \frac{\ln a - \ln A}{\sigma_{\ln A}} \tag{12}$$

where *"A"* is a ground motion parameter will exceed a particular value *"a"*. Probability of *"A"* exceed *"a"* *P*(A>*a*|*m*,*r*) = *p*(*z**), see Figure 4, can be looked for in normal distribution table.

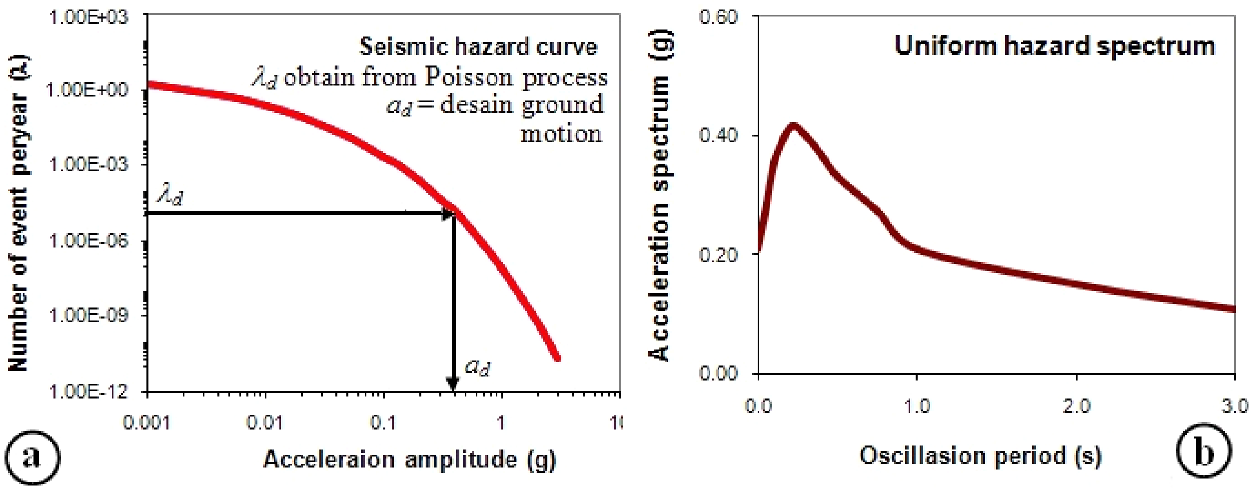

Figure 4. Example of seismic hazard curve (a) and uniform hazard spectrum (b)

4.5. Seismic Hazard Curve

Frequency of a seismic event $\lambda(A>a)$ for n number of earthquake sources was accounted for by the function:

$$\lambda_A(a) = \sum_{i=1}^{n}\{v_i \int_M \int_R P(A > a)|m,r) f_M(m) f_R(r) dr dm\} \tag{13}$$

where R is distance rupture-to-site, and M is magnitude. Relation between acceleration a and $\lambda(A>a)$ called seismic hazard curve (Figure 4-a).

According to ground motion prediction relation and its period (*the attenuation function*) so based on Equation 9 and 10 can be accounted for a spectrum of ground motion parameter (e.g. acceleration ground motion) in probabilistic framework as a curve. The curve was called uniform hazard spectrum (Figure 4-b).

4.6. Result of Seismic Hazard Calculation

The Alana Hotel Building in Yogyakarta, with coordinate points of 7^0 10' 20'' latitude and 110^0 24' 49'' longitude, underwent seismic hazard computation using the PSHA procedure. Calculation was carried out based on 2% probability of exceeding (PE) in 50 years, the site with rock conditions (the site is bedrock), and the seismic sources and parameters as in Tables 1 and 2. Figure 3 displays the results of a probabilistic seismic hazard analysis in bedrock with a 2% PE in 50 years, based on the data in Tables 1 and 2, and Equation 10. Figure 2 was called a Uniform Hazard Spectrum (UHS). The spectrum is used as a target spectrum in the spectral matching calculation.

Table 1. Subduction source zones and parameters

Subduction source name	Magnitude (M_{max})	Rate (v) (event/year)	Parameter	
			a	*b*
Java-1 Megathrust	8.0	3.2359	5.76	1.05
Java-1 Benioff	8.1	3.2359	5.76	1.05
Java-2 Megathrust	8.1	4.3652	6.14	1.10
Java-2 Benioff	8.1	4.3652	6.14	1.10
Java-3 Megathrust	8.1	6.4565	6.81	1.20
Java-3 Benioff	8.1	6.4565	6.81	1.20

Table 2. Fault sources and parameters

Fault name	Slip-rate (mm/year)	Magnitude (M_{max})	Rate (v) (event/year)	Parameter	
				b	*a*
Bumi Ayu	5.0	6.7	0.2851	1	4.4550
Pati	4.0	6.8	0.2583	1	4.4121
Lasem	0.5	6.5	0.0213	1	3.3290
Opak-Jogja	2.4	6.8	0.1159	1	4.0642

According to the Indonesian National Standard (SNI-2019) [11] about the seismic design so, the Figure 5 can be used in practical purpose is 2/3 of the uniform hazard spectrum Figure 5. Therefore, the form of 2/3 of uniform hazard spectrum can be seen in Figure 6.

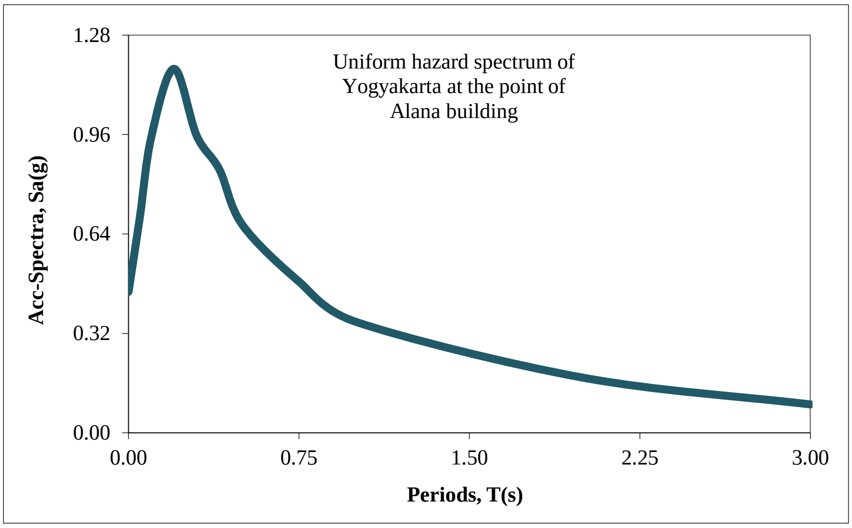

Figure 5. Uniform hazard spectrum of the site in 2% PE in 50 years

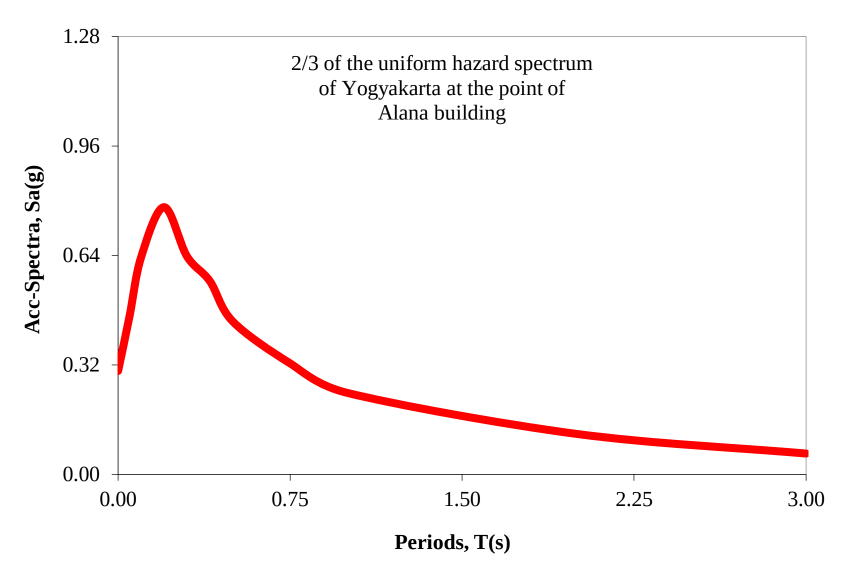

Figure 6. 2/3 of the uniform hazard spectrum of the site in 2% PE in 50 years

5. Design Response Spectrum of SNI 2019 Code

To develop the design spectrum of the SNI 2019 code [11] for the study site, the drill log result that is correlated between normal penetration test (NSPT) and the depth is used.

We determine the site's soil condition based on ASCE 2013 (ASCE 7-10) and drilling results. The ACSE code 7-10 provides a table that correlates the site class with the shear wave velocity (Vs), the Normal-Soil Penetration Test (N-SPT), and the undrained shear strength (Su); refer to Table 3. Figure 7 displays the drill log for the Alana Hotel Building. Based on the drill results, Figure 6 determines that the soil site class of the Alana Hotel is D, with a mean N-SPT of 15.4. Therefore, we assume that the research site's soil condition is class D soil.

Table 3. Site classification

Site Class	Vs	N	Su
A Hard rock	>5000 ft/s >1500 m/s	Not applicable	Not applicable
B Rock	2500 to 5000 ft/s 760 to 1500 m/s	Not applicable	Not applicable
C Very dense soil and soft rock	1200 to 2500 ft/s 370 to 760 m/s	>50 -	>2000 PSF >100 kPa
D Stiff soil	600 to 1200 ft/s 180 to 370 m/s	15 to 50 -	1000 to 2000 PSF 50 to 100 kPa
E Soil	<600 ft/s <180 m/s	<15 -	<1000 PSF <50 kPa
	Any profile with more than 10 ft (3 m) of soil having characteristic: * Plasticity index (PI) > 20 * Moisture content, w > 40% * Un-drained shear strength, Su < 500 PSF		
F Soil requiring the site-specific evaluation	a. Soil vulnerable to potential failure or collapse b. Peats and/or highly organic clays c. Very high plasticity clays d. Very thick soft/medium clays		

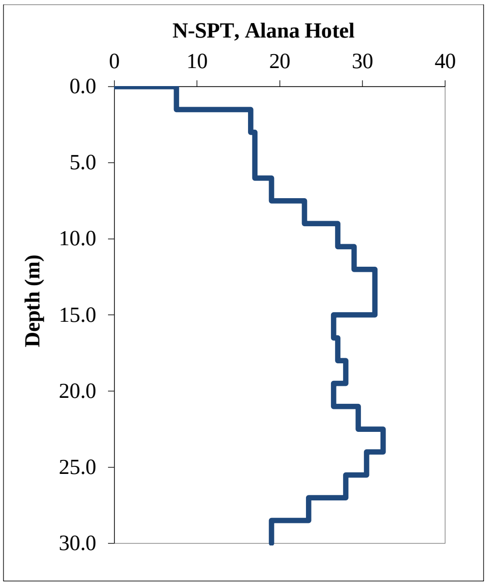

Figure 7. Drill log result of Alana Hotel structure

The design response spectrum of the SNI 2019 code [11] is developed based on soil site class D, the seismic hazard map of Indonesia 2019, Figures 8 and 9, Tables 4 and 5, and Equations 14 and 22. From the Figures 8 and 9, Ss = 1.2149 g and S_1 = 0.5315. Based on the Ss and S_1 values, and Tables 4 and 5, Fa = 1.0140 and Fv = 1.7685 are found.

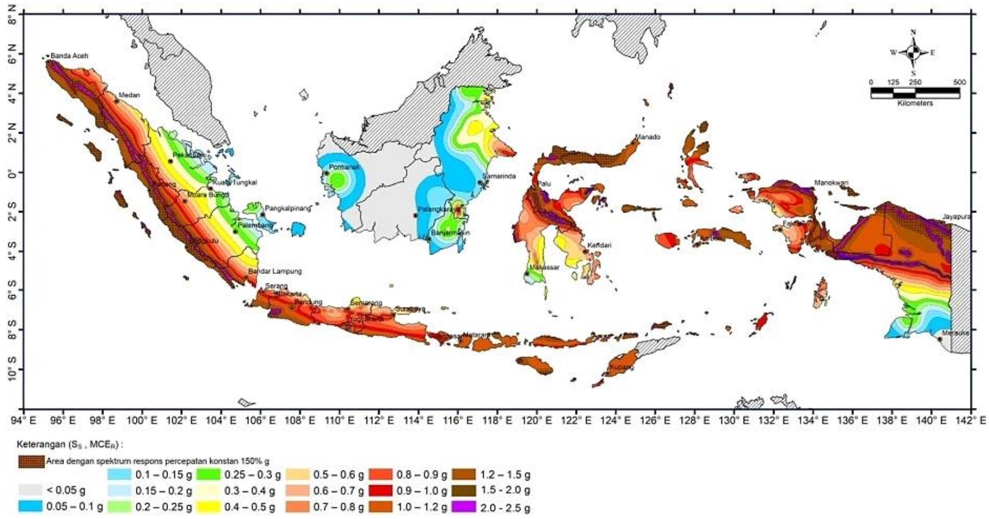

Figure 8. Indonesian seismic hazard map for 0.2s periods

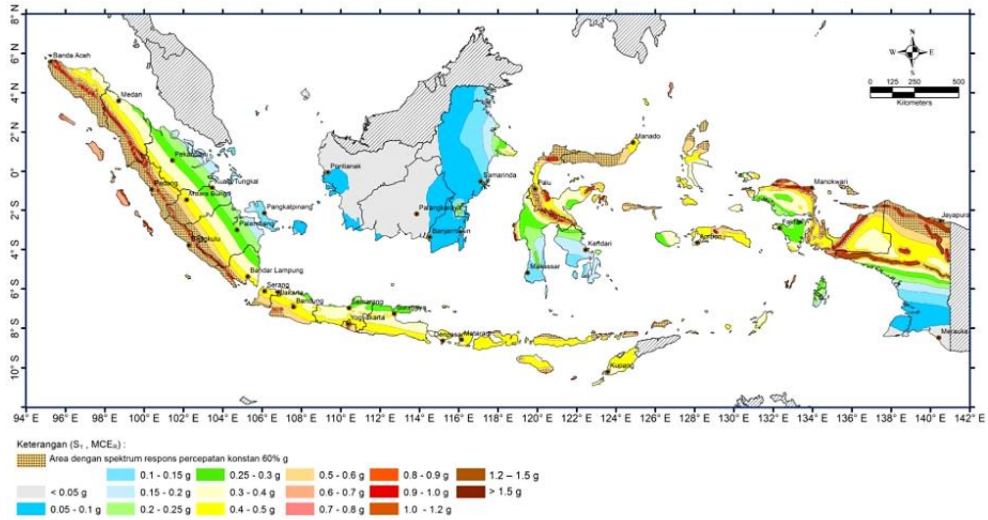

Figure 9. Indonesian seismic hazard map for 1.0s periods

Table 4. Table to determine the amplification factor Fa

Site Class	Ss	Ss	Ss	Ss	Ss	Ss
	0.25	0.5	0.75	1.0	1.25	1.5
			Fa			
A	0.8	0.8	0.8	0.8	0.8	0.8
B	0.9	0.9	0.9	0.9	0.9	0.9
C	1.3	1.3	1.2	1.2	1.2	1.2
D	1.6	1.4	1.2	1.1	1	1
E	2.4	1.7	1.3	1.1	0.9	0.8
F	a	a	a	a	a	a

Table 5. Table to determine the amplification factor Fv

Site Class	Ss	Ss	Ss	Ss	Ss	Ss
	0.1	0.2	0.3	0.4	0.5	0.6
			Fv			
A	0.8	0.8	0.8	0.8	0.8	0.8
B	0.8	0.8	0.8	0.8	0.8	0.8
C	1.5	1.5	1.5	1.5	1.5	1.4
D	2.4	2.2	2	1.9	1.8	1.7
E	4.2	3.3	2.8	2.4	2.2	2
F	a	a	a	a	a	a

From Ss, S_1, Fa, and Fv value can be computed some parameters to developed the design spectrum as follow:

$$S_{MS} = Fa\ Ss = 1.2320g \tag{14}$$

$$S_{M1} = Fv\ S_1 = 0.9400g \tag{15}$$

$$S_{DS} = 2/3\ S_{MS} = 0.8213g \tag{16}$$

$$S_{D1} = 2/3\ S_{M1} = 0.6266g \tag{17}$$

$$T_S = S_{D1}/S_{DS} = 0.7630s \tag{18}$$

$$T_0 = 0.2*T_S = 0.1526s \tag{19}$$

For $T < T_0$ the spectral acceleration (Sa) is,

$$Sa = S_{DS}\ (0.4+0.6\ T/T_0) \tag{20}$$

For $T_0 \leq T \leq T_S$ the spectral acceleration (Sa) is,

$$Sa = S_{DS} \tag{21}$$

For $T > T_S$ the spectral acceleration (Sa) is,

$$Sa = S_{D1}/T \tag{22}$$

where S_S is mapped MCER, 5% damped, spectral response acceleration parameter at short periods, S_1 mapped MCER, 5% damped, spectral response acceleration parameter at a period of 1 sec, F_a short-period site coefficient (at 0.2-s period), F_v long-period site coefficient (at 1.0-s period), SMS the MCER, 5% damped, spectral response acceleration parameter at short periods adjusted for site class effects, S_{M1} the MCER, 5% damped, spectral response acceleration parameter at a period of 1 s adjusted for site class effects, S_{DS} design, 5% damped, spectral response acceleration parameter at short periods, S_{D1} design, 5% damped, spectral response acceleration parameter at a period of 1 sec, and T the fundamental period of the building.

With the use of Sa and T values above, the design spectrum can be drawn, such as in Figure 10.

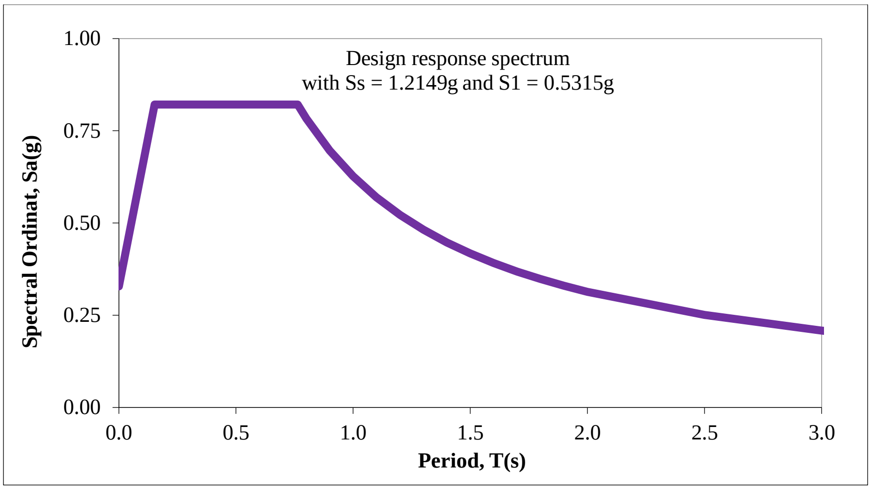

Figure 10. SNI 2019 code response spectrum

Figures 5 and 10 is used a target spectrum to develop the new ground motion design by the spectral matching process.

6. Actual Time History

The time history acquired from alternative sources, such as the PEER source, is designated as the actual time history. This work aims to construct a unique time history of earthquake ground motion, drawing on actual measurement data from the 1957 San Francisco earthquake in the USA, which occurred at a rock location (Figure 11).

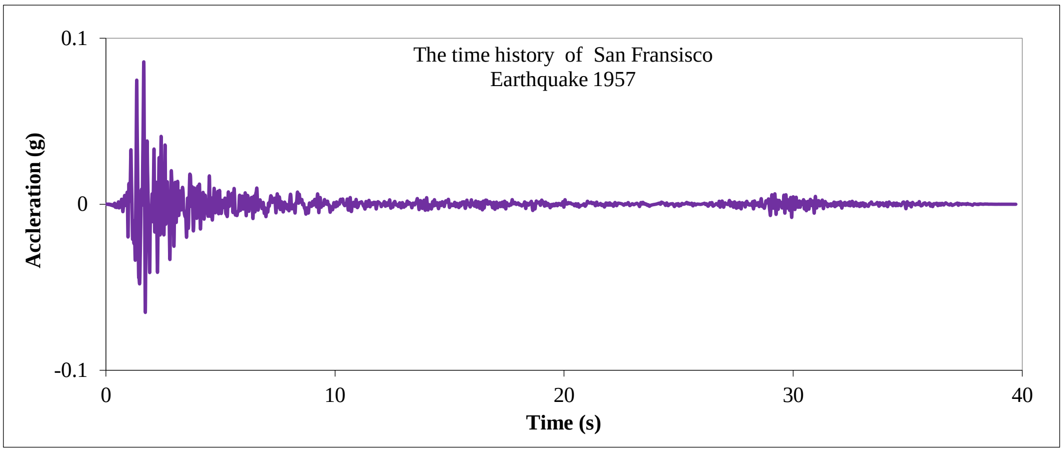

Figure 11. Time history of San Fransisco earthquake USA 1957

Response spectra of the time history of Figure 11 is in Figure 12.

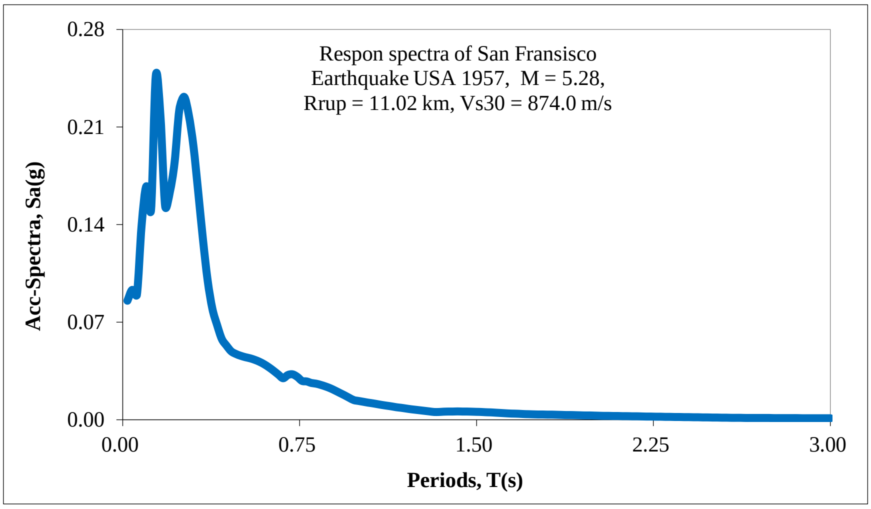

Figure 12. Response spectra of the earthquake wave of the Figure 11

7. Wave Propagation

To obtain the earthquake wave at the soil surface as a time history, the earthquake wave depicted in Figure 11 must be propagated from the bedrock to the soil surface by ground response analysis. The analysis examines the vertical propagation of the shear wave from bedrock to the ground surface in a one-dimensional layered system. Bardet & Tobita [22] created a computer program for non-linear site response analysis of stratified soil deposits, employing the theory. The equation employed for the analysis calculation is as follows:

$$\rho \frac{\partial^2 d}{\partial t^2} + \eta \frac{\partial d}{\partial t} = \frac{\partial \tau}{\partial z} \tag{23}$$

where ρ is the soil unit mass, d is the horizontal displacement, z is the depth, t is the time, τ is the shear stress, and η is a mass-proportional dumping coefficient. But in the study is utilized the DEEPSOIL program computer to propagate and find the earthquake wave in the soil surface.

8. Spectral Matching

The artificial time history should be developed using the spectral matching approach. Spectral matching can be performed by utilizing the target spectrum as the objective and the actual response spectrum as the matched spectrum. The matching process may be executed in the frequency domain. The outcome of spectral matching is a fake time history and a novel response spectrum referred to as the matching spectrum. Nicolaou [18] delineates the spectral matching technique within the frequency domain as follows:

a). Select the target spectrum $\{S_a^{target}(T)\}$

b). Kindly choose the chronological record for the match (TH_{actual})

c). Compute the $\{S_a^{actual}(T)\}$ actual response spectrum with equivalent attenuation to that of the target spectrum.

d). Determine the ratio of the actual spectrum to the intended spectrum {SPR(T)}, refer to Equation 24.

e). Compute the real Fourier spectrum $\{F_{actual}(\omega)\}$ from actual time history $\{TH_{actual}(t$ with the discrete Fourier analysis algorithm (DFA).

f). Use the frequency domain SPR (ω) in the form of Equation 25 to filter the actual Fourier series with the Fourier filtered result [$F_{filtered}(\omega)$] in the form of Equation 26.

g). Compute the time history with the frequency characteristics in step f, and use the Fourier inverse to determine the TH(t) of the target spectrum.

Compute the mean error (deviation of the TH(t) response spectrum from the target spectrum). If the designated tolerance limits allow the error in this step, the calculation is considered complete. If the error is unacceptable, repeat steps (b) through (h) until the error is acceptable.

$$SPR(T) = \frac{S_a^{t\,arg\,et}(T)}{S_a^{aktual}(T)} \tag{24}$$

$$FILT(\omega) = \begin{cases} 1 & \omega < \omega_{min} \\ SPR(\omega) & \omega_{max} < \omega < \omega_{max} \\ 1 & \omega > \omega_{max} \end{cases} \tag{25}$$

$$F_{filtred}(\omega) = FILT(\omega)\, F_{aktual}(\omega) \tag{26}$$

The variables T and ω denote the spectral period (wave period) and cyclic frequency, respectively. The variables ω_{min} and ω_{max} denote the smallest and maximum matching cyclic frequencies, respectively.

Estimating the error by matching in the frequency domain can be accomplished similarly to matching in the time domain. Consequently, Equation 27 encompasses the formula for calculating the error in the frequency domain.

$$|Error|_N\% = 100 \times \frac{\sqrt{\int_{T_A}^{T_B} (S_a^{scaled} - S_a^{t\,arg\,et})^2 dT}}{\int_{T_A}^{T_B} S_a^{t\,arg\,et} dT} \tag{27}$$

$S_a^{scaled}(T)$ denotes the response spectrum of the actual time history $\{TH_{actual}(t)\}$ produced by the spectral match in the frequency domain, while $S_a^{target}(T)$ represents the target spectrum.

The matching process in this instance relies on the real-time history depicted in Figure 11 and the response spectrum illustrated in Figure 12. Figures 6 and 10 illustrated the target spectrum for the match.

8.1. PSHA Time History

Spectral matching is conducted between response spectra Figure 13 and the target spectrum is Figure 6. The matching results of the case are shown in Figures 13 and 14. Figure 13 is the spectral matching result in form of the response spectra and Figure 14 is the spectral matching result in form of the time history.

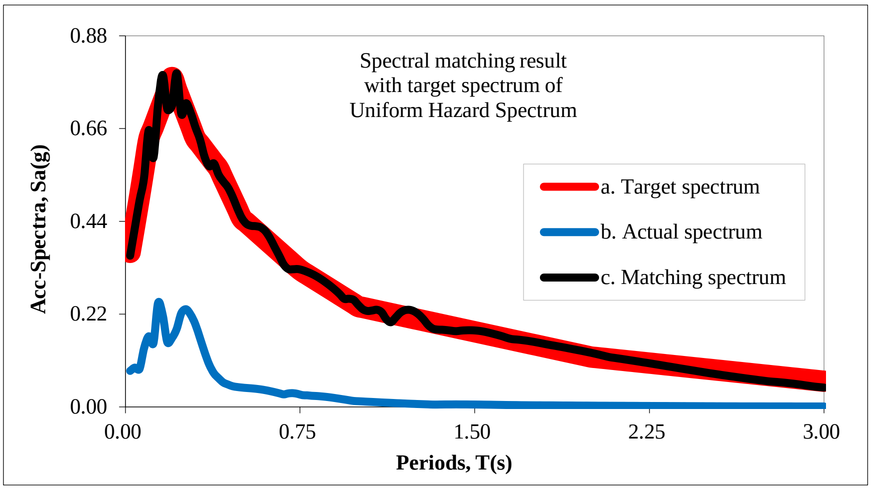

Figure 13. Response spectra of matching result between Figure 12 to Figure 6

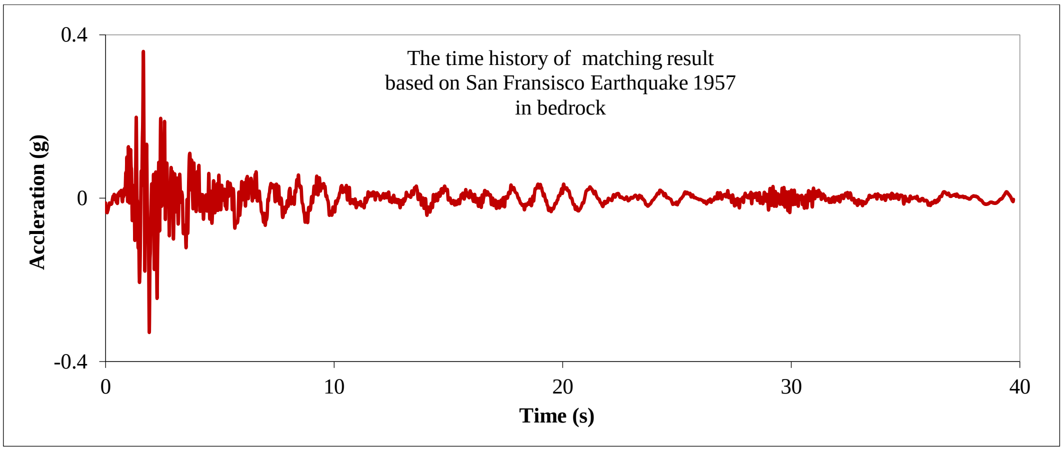

Figure 14. Time history of matching result based on Figure 11 in bedrock

Figure 14 is mentioned as the time history that developed probabilistically because the target spectrum that was used to form the time history developed with probabilistic seismic hazard analysis.

The DEEPSOIL computer program then propagates the earthquake wave (Figure 14) to the ground surface. Figure 15 displays the time history of the propagated result. Time history Figure 15 is called the PSHA time history.

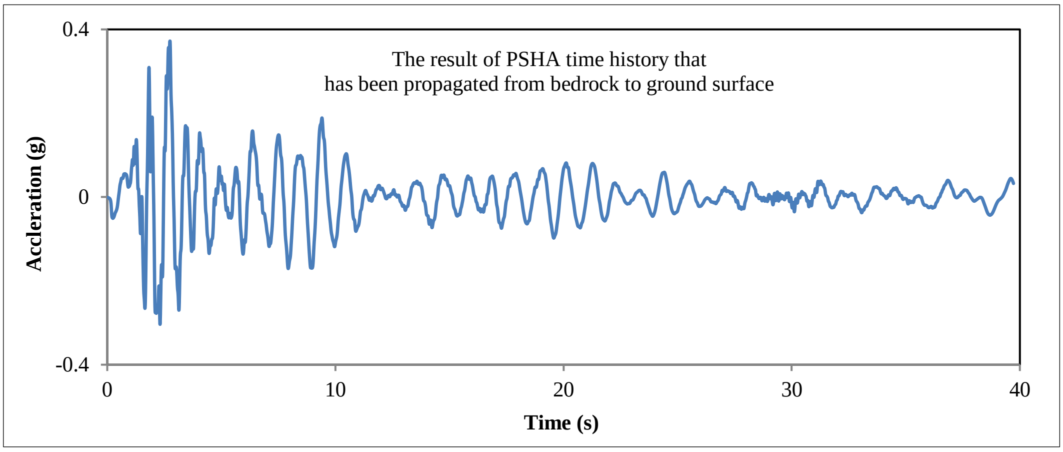

Figure 15. Result of the time history propagated from bedrock to ground surface

8.2. Code Time history

To develop the time history in this case, spectral matching is conducted on the ground surface based on the target spectrum. Figure 10. Prior to processing the spectral matching, Figure 12 propagates the time history of the 1957 San Francisco earthquake from the bedrock to the ground surface. Result of the time history propagation of Figure 11 to the ground surface in Figure 16.

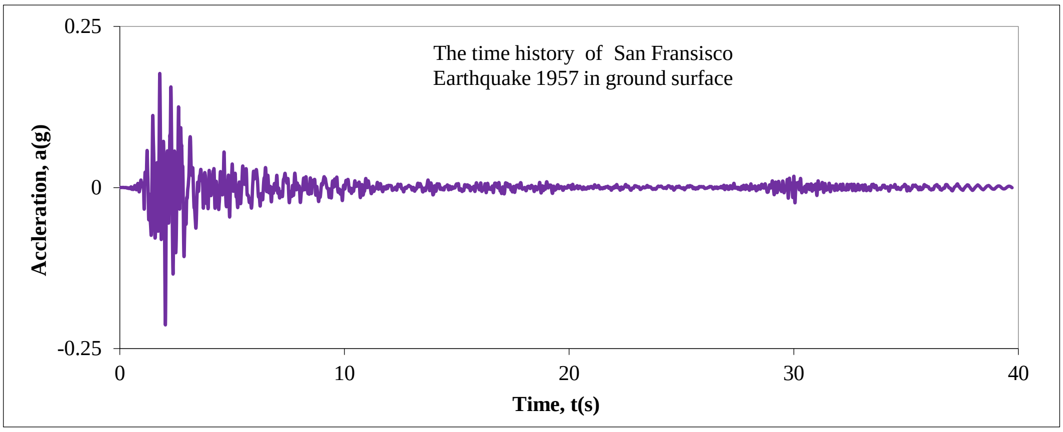

Figure 16. Time history of propagation result of San Fransisco earthquake USA 1957 from bedrock to the ground surface

Response spectra of the time history Figure 16 is shown in Figure 17.

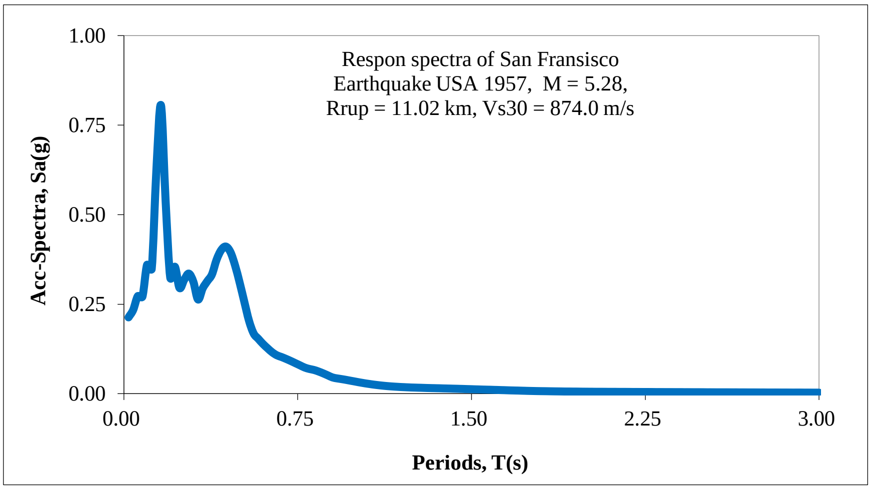

Figure 17. Response spectra of the time history

Spectral matching result between response spectra Figure 17 and target spectrum Figure 10 is shown in Figures 18 and 19. Figure 18 is the spectral matching result in form of the response spectra and Figure 19 is the spectral matching result in form of the time history.

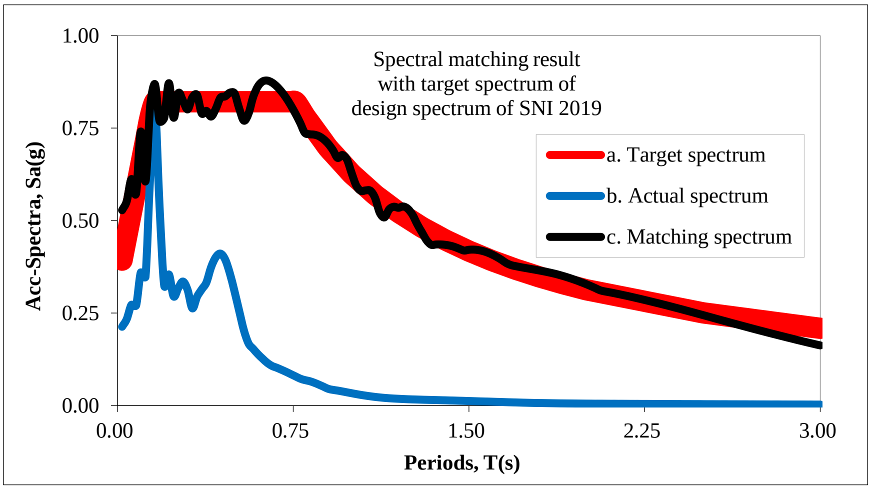

Figure 18. Response spectra of matching result between Figure 17 to Figure 10

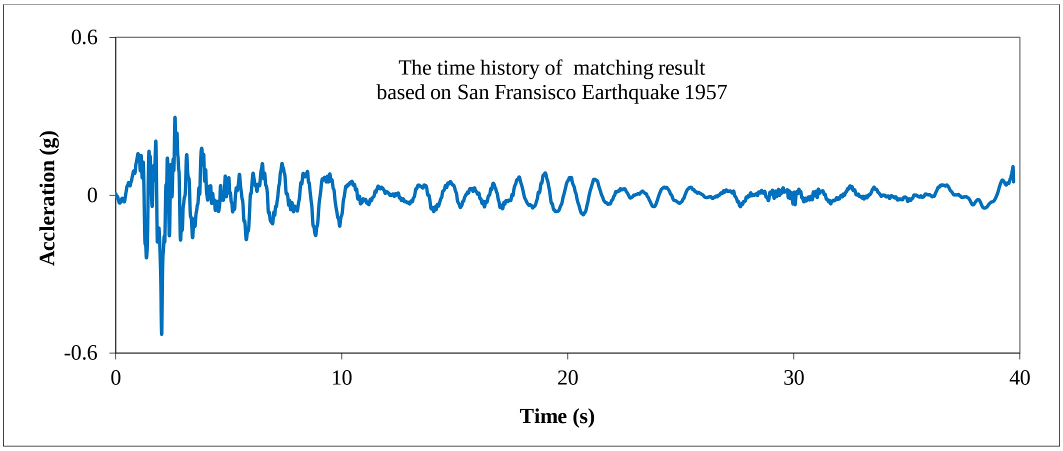

Figure 19. Time history of matching result between Figure 18 to Figure 11

Time history Figure 19 is called the *SNI 2019 time-history*. Time history in Figures 15 and 19 are used as a basis to analyze the structural response of the Alana Hotel structure in the next paragraph.

9. Structural Analysis

The Alana Hotel structure in Yogyakarta, Indonesia (Figure 1) undergoes structural analysis. The analysis was utilized to evaluate the Alana Hotel structure's (Figure 20) response to the earthquake acceleration wave, which is the time history of Figures 15 and 19. The Structural Analysis Program, PERFORM 3D, was used to shake the Alana Hotel structure. The result of the analysis is in Figure 21.

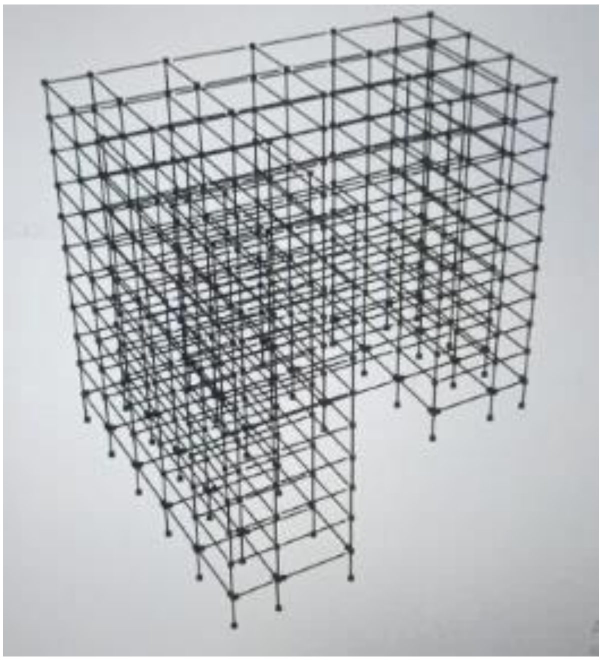

Figure 20. The structure few of the Alana Hotel Building

Figure 21 explains that the displacement values provided by the two time histories are not significantly different. The two time histories are not significantly different, which leads to the displacement pattern. From the second story to the fifth story, and from the tenth story to the twelfth story, the PSHA time-history displacement is greater than the SNI 2019 time-history. Conversely, from the fifth story to the tenth story, the displacement of the PSHA time history is slightly less than that of the SNI 2019 time history. It is known that the maximum acceleration of the SNI 2019 time history is greater than the maximum acceleration of the PSHA time history. Therefore, it can be said that the maximum acceleration of a time history does not always give the greater displacement compared to the other time history. This study found that the SNI 2019 time history's mean displacement is 0.0314 smaller than the PSHA time history, with a maximum displacement of 0.321 mm.

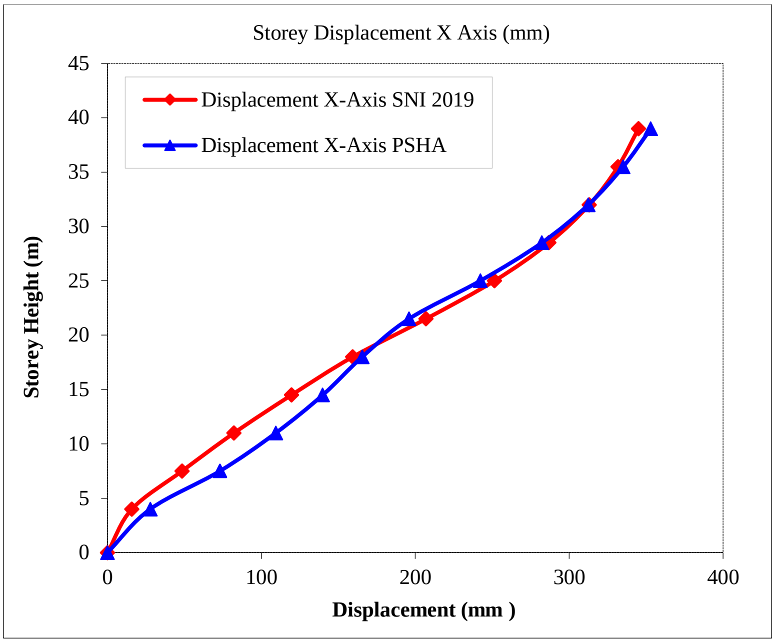

Figure 21. Structure displacement on X-direction of the structure Figure 21

This study also computes the drift parameter. Figure 22 shows a curve that correlates the drift ratio with the constructed structure story. The SNI 2019 code indicates that the maximum drift ratio should be less than 2% [11]. The structure analysis reveals that the maximum drift ratio for the two time-histories is 0.0136 (1.36%), which is less than 2%. Therefore, it can be said that the structure is safe to drift ratio condition. In the whole, it can be stated that the structure is safe from the collapse caused by displacement and safe to be occupied.

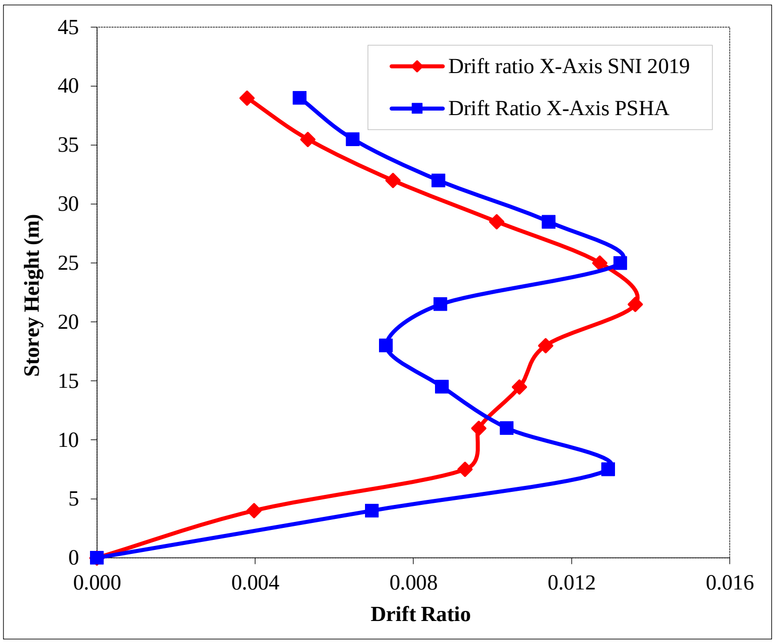

Figure 22. Drift ratio curve

10. Discussion

Certain purposes necessitate the development of an earthquake's artificial ground motion (earthquake acceleration time history). In the study, two time histories have been developed from the single time history in bedrock, that is, the time history of the San Francisco earthquake of 1957 (called the source time history). The development of first-time history relies on probabilistic seismic hazard analysis in bedrock. The PSHA yields a response spectrum known as the uniform hazard spectrum. This spectrum is used as a target spectrum to conduct the spectral matching in the frequency domain. The result of the spectral matching is a time history (Figure 14). Figure 15 represents the propagation of this time history to the ground surface. The development of second-time history relies on the SNI 2019 code. The propagation of the source's time history from bedrock to the ground surface occurs first. We match the propagated time history in the ground surface (Figure 16) to the target spectrum, which is the design response spectrum. Figure

10. Figure 19 displays the time history resulting from the spectral matching process. The time history While the visual pattern of Figures 15 and 19 is nearly the same, the response spectra of the two time histories differ significantly. Figure 13 illustrates the tapering response spectra of the time history in Figure 15, whereas Figure 19 displays blunt serrated response spectra. The time history of Figure 15 has a maximum acceleration of a_{max}=0.3713g, which is smaller than the maximum acceleration of Figure 19's a_{max}=0.5290g. The maximum acceleration differences show that the target spectral acceleration value of the design spectrum is greater than the target spectral acceleration value of the uniform hazard spectrum of PSHA.

The structure analysis reveals that the SNI 2019 time history, which has a maximum acceleration of a_{max}= 0.5290 g, yields a mean displacement of 0.0345 m. This is less than the PSHA time history, which has a displacement of 0.0353 m and a maximum acceleration of a_{max}=0.3713g. According to the drift ratio parameter, a time history with a greater maximum acceleration does not always result in a greater mean displacement compared to a time history with a smaller maximum acceleration.

11. Conclusion

This study generated two seismic activities on the ground surface. We refer to this ground movement as the time history of earthquake acceleration. Created the initial time history using probabilistic methods, and the next one adhered to the 2019 SNI code. Used the two time histories to evaluate the structural response of the Alana Hotel in Yogyakarta, Indonesia. The structural analysis results indicate no significant differences in structural deformation. The PSHA method shows a deformation of 353 mm, whereas the SNI method shows a deformation of 345 mm. The permissible deformation according to SNI is 2% of the floor height, which is 780 mm. Artati's research aligns with this, demonstrating that the earthquake vibrations produced using PSHA and SNI exhibit minimal differences. However, Artati uses earthquake vibrations to figure out how likely it is that a soil will liquefy.

11.1. Recommendation

The study about structural analysis associated with the earthquake vibration, and the earthquake engineering, there are still many opportunities to do the research, therefore, for the doctoral student in civil engineering department of Islamic University of Indonesia can carry out research about the topic.

12. Declarations

12.1. Author Contributions

Conceptualization, L.M. and P.; methodology, W.P.; software, P.; validation, L.M., Y.M., and W.P.; formal analysis, P.; investigation, P.; resources, W.P.; data curation, Y.M.; writing—original draft preparation, P.; writing—review and editing, W.P.; visualization, Y.M.; supervision, W.P.; project administration, P.; funding acquisition, P. All authors have read and agreed to the published version of the manuscript.

12.2. Data Availability Statement

The data presented in this study are available on request from the corresponding author.

12.3. Funding

The authors received no financial support for the research, authorship, and/or publication of this article.

12.4. Acknowledgements

The author gratefully acknowledges the Head of the Doctoral Program in the Civil Engineering Department at the Islamic University of Indonesia for their support and encouragement in conducting this research.

12.5. Conflicts of Interest

The authors declare no conflict of interest.

13. References

[1] Saputro I.T. (2016). Evaluation of the response of multi-storey building structures using time history based on the PSHA method with shallow crustal earthquake sources. Master Thesis, Magister Teknik Sipil Univesitas Islam Indonesia Yogyakarta, Indonesia. (In Indonesian).

[2] Pawirodikromo, W. (2019). On the capacity of high, moderate and low earthquake frequency content to cause global drift ratio at level-2 of structural performance. MATEC Web of Conferences, 258, 05027. doi:10.1051/matecconf/201925805027.

[3] Utomo, J. (2019). Seismic performance evaluation of special moment frame using Perform 3D. Journal Media Komunikasi Teknik Sipil, 25(1), 27–37.

[4] Widodo, P. (2023). Contibution of normalized Hysteritic Energy to damage Index in inelastic response of SDOF Structure due to earthquake. Journal Teknisia, 28(01), 055–069.

[5] Bayati, Z., & Soltani, M. (2016). Ground motion selection and scaling for seismic design of RC frames against collapse. Earthquake and Structures, 11(3), 445–459. doi:10.12989/eas.2016.11.3.445.

[6] Irsyam, M., & Hendriyawan, D. AD (2003) Seismic Hazard Assessment LNG Storage Tank Terminal Teluk Banten. Report of Seismic Hazard Study, Bandung, Indonesia.

[7] Pawirodikromo, W., Makrup, L., Teguh, M., & Anggit, M. (2019). Bidirectional and Directivity Effect Identifications of Synthetic Ground Motions At Selected Site in Yogyakarta City , Indonesia. International Journal of Civil Engineering and Technology, 10(11), 149–166.

[8] Artati, H. (2024). Liquefaction Potential Using a State Parameter Approach Based on Earthquake Peak Ground Acceleration Generated From Codes, Deterministic and Probabilistic Seismic Hazard Analysis. Dissertation Faculty of Civil Engineering, Islamic University of Indonesia, Yogyakarta, Indonesia.

[9] Nugroho, N. S., Erizal1, Putra, H. (2021). Structure evaluation of building based on the earthquake response acceleration spectrum of the SNI 03-1726-2019. IOP Conference Series: Earth and Environmental Science, 871(1), 012013. doi:10.1088/1755-1315/871/1/012013.

[10] Rocky, M. (2023). Earthquake Hazard Probability Analysis Of Indonesia's New Capital City. Journal Media Komunikasi Teknik Sipil, 28(2), 284–291.

[11] SNI 1726. (2019). Earthquake Resistance Planning Procedures for Building and Non-Building Structures Badan Standarisasi Nasional (BSN), Jakarta, Indonesia. (In Indonesian).

[12] Kramer, S.L. (1996) Geotechnical Earthquake Engineering. Prentice-Hall, New Jersey, United States.

[13] Gutenberg, B., & Richter, C. F. (1944). Frequency of earthquakes in California*. Bulletin of the Seismological Society of America, 34(4), 185–188. doi:10.1785/bssa0340040185.

[14] Sadigh, K., Chang, C. Y., Egan, J. A., Makdisi, F., & Youngs, R. R. (1997). Attenuation relationships for shallow crustal earthquakes based on California strong motion data. Seismological Research Letters, 68(1), 180–189. doi:10.1785/gssrl.68.1.180.

[15] Youngs, R. R., Chiou, S. J., Silva, W. J., & Humphrey, J. R. (1997). Strong ground motion attenuation relationships for subduction zone earthquakes. Seismological Research Letters, 68(1), 58–73. doi:10.1785/gssrl.68.1.58.

[16] Boore, D. M., & Atkinson, G. M. (2008). Ground-motion prediction equations for the average horizontal component of PGA, PGV, and 5%-damped PSA at spectral periods between 0.01s and 10.0s. Earthquake Spectra, 24(1), 99–138. doi:10.1193/1.2830434.

[17] ERPI. (1986). Seismic Hazard Methodology for the Central and Eastern United States. Electric Power Research Institute (ERPI), Palo Alto, United States.

[18] Nikolaou, A. S. (1998). A GIS platform for earthquake risk analysis. State University of New York at Buffalo. Ph.D. Thesis, State University of New York at Buffalo, Buffalo, United States.

[19] Cornell, C. A., & Vanmarcke, E. H. (1969). The major influences on seismic risk. Proceedings of the fourth world conference on earthquake engineering, 13-18 January, 1969, Santiago, Chile.

[20] Youngs, R. R., & Coppersmith, K. J. (1986). Implications of fault slip rates and earthquake recurrence models to probabilistic seismic hazard estimates. International Journal of Rock Mechanics and Mining Sciences & Geomechanics Abstracts, 23(4), 125. doi:10.1016/0148-9062(86)90651-0.

[21] McGuire, R. K. (1976). EQRISK: Evaluation of earthquake risk to site. Open File Report, 76, 67, A Computer Program Distributed by NISEE/Computer Applications, Geological Survey, United States Department of the Interior, Washington, United States.

[22] Bardet, J. P., & Tobita, T. (2001). NERA: a computer program for nonlinear earthquake site response analyses of layered soil deposits. Department of Civil Engineering, University of Southern California, California, United States.